

Spectrum and thermal fluctuations of a microcavity polariton Bose-Einstein condensate

D. Sarchi* and V. Savona

Institute of Theoretical Physics, Ecole Polytechnique Fédérale de Lausanne EPFL, CH-1015 Lausanne, Switzerland

(Dated: February 5, 2008)

The Hartree-Fock-Popov theory of interacting Bose particles is developed, for modeling exciton-polaritons in semiconductor microcavities undergoing Bose-Einstein condensation. A self-consistent treatment of the linear exciton-photon coupling and of the exciton non-linearity provides a thermal equilibrium description of the collective excitation spectrum, of the polariton energy shifts and of the phase diagram. Quantitative predictions support recent experimental findings.

PACS numbers: 71.36.+c, 71.35.Lk, 42.65.-k, 03.75.Nt

A major advance in the research on quantum fluids was made with the recent experimental observation of quantum degeneracy and off-diagonal long-range order (ODLRO), in a gas of exciton-polaritons in a semiconductor microcavity [1, 2, 3]. Bose-Einstein condensation (BEC) is the most appealing way of interpreting these findings. However, the **2-D** nature of the system, the presence of disorder, the hybrid exciton-photon composition of polaritons, and the composite nature of excitons, call for models that account for the peculiar aspects of the polariton gas. Along this line, recent theoretical works have been successful in describing many specific aspects of the system. Disorder at the quantum well interfaces, in particular, was accounted for by a BCS-like theory in which bound excitons were modeled as particle-hole excitations coupled to the photon field [4, 5, 6]. For strong exciton disorder, this theory models the density dependence of the polariton spectrum and shows how the linear optical response can probe successfully the phase transition. More generally, in presence of localization, the lower-energy region of the density of states is modified with respect to an ideal 2-D system [7, 8], making BEC of a trapped polariton gas the most suited description of the system. Finally, the short radiative lifetime of polaritons results in non-equilibrium effects [6, 9, 10, 11, 12, 13, 14], leading to condensate depletion [14] and to a modified excitation spectrum [6, 13]. These effects should however be weak at densities above the condensation threshold [2], and are expected to be negligible for a polariton lifetime longer than 10 ps.[24] Very recent measurements clearly show that thermal equilibrium polariton BEC can indeed be achieved [3]. In spite of the high relevance of the existing theoretical frameworks, a basic question remains still unanswered. Are the experimental findings correctly interpreted in terms of a quantum field theory of interacting bosons? Such a theory should account self-consistently for the linear coupling between two Bose fields – photons and excitons – and for the Coulomb and Pauli non-linearities arising from the composite nature of excitons.

In this Letter, we answer this question by generalizing the Hartree-Fock-Popov (HFP) [15, 16] theory of

BEC to the case of two coupled Bose fields. In order to address the fundamental thermodynamical properties of the polariton gas, we assume thermal equilibrium – as was done in previous works based on non-bosonic models [4, 5] – and discuss kinetic effects elsewhere [14]. The system, including the Coulomb and Pauli non-linear exciton terms, is described within an effective boson Hamiltonian [17, 18, 19], valid well below the exciton Mott density. We derive coupled equations for the condensate wave function and the field of excitations, and study the solutions for parameters modeling a recent experiment [2]. We discuss the collective excitation spectrum, the density-dependent energy shifts, the onset of off-diagonal long-range order and the phase diagram. Our analysis provides a generally good account of the experimental findings, in particular by reproducing the measured critical density and the energy shifts of the two polariton modes.

Let us introduce the exciton and photon operators \hat{b}_k and \hat{c}_k , obeying Bose commutation rules.[25] The polariton Hamiltonian then reads

$$\hat{H} = \hat{H}_0 + \hat{H}_R + \hat{H}_x + \hat{H}_s, \quad (1)$$

where $\hat{H}_0 = \sum_{\mathbf{k}} \epsilon_{\mathbf{k}}^x \hat{b}_{\mathbf{k}}^\dagger \hat{b}_{\mathbf{k}} + \epsilon_{\mathbf{k}}^c \hat{c}_{\mathbf{k}}^\dagger \hat{c}_{\mathbf{k}}$ is the non-interacting term, $\hat{H}_R = \hbar \Omega_R \sum_{\mathbf{k}} (\hat{b}_{\mathbf{k}}^\dagger \hat{c}_{\mathbf{k}} + h.c.)$ describes the linear exciton-photon coupling, and $\hat{H}_x = \frac{1}{2} \sum_{\mathbf{k}, \mathbf{k}', \mathbf{q}} v_x(\mathbf{k}, \mathbf{k}', \mathbf{q}) \hat{b}_{\mathbf{k}+\mathbf{q}}^\dagger \hat{b}_{\mathbf{k}'-\mathbf{q}}^\dagger \hat{b}_{\mathbf{k}'} \hat{b}_{\mathbf{k}}$ is an effective 2-body exciton Hamiltonian, modeling both Coulomb interaction and the effect of Pauli exclusion on electrons and holes. The term $\hat{H}_s = \sum_{\mathbf{k}, \mathbf{k}', \mathbf{q}} v_s(\mathbf{k}, \mathbf{k}', \mathbf{q}) (\hat{c}_{\mathbf{k}+\mathbf{q}}^\dagger \hat{b}_{\mathbf{k}'-\mathbf{q}}^\dagger \hat{b}_{\mathbf{k}'} \hat{b}_{\mathbf{k}} + h.c.)$ models the effect of Pauli exclusion on the exciton oscillator strength [17, 19], which decreases for increasing exciton density [21]. We account for the full momentum dependence of $v_x(\mathbf{k}, \mathbf{k}', \mathbf{q})$ and $v_s(\mathbf{k}, \mathbf{k}', \mathbf{q})$ [17, 19]. They vanish at large momenta, preventing the ultraviolet divergence typical of a contact potential [22].[26] For clarity, however, we use the short form $v_x(\mathbf{k}, \mathbf{k}', \mathbf{q}) \rightarrow v_x$ and $v_s(\mathbf{k}, \mathbf{k}', \mathbf{q}) \rightarrow \hbar \Omega_R / n_s$ in what follows, where n_s is the saturation density of the exciton oscillator strength [17].

As non-interacting exciton and photon modes, we assume states in a square box of area A with periodic

boundary conditions. In real microcavities, interface fluctuations affect the photon modes, resulting in a disorder potential and in polariton localization over a few μm [2]. For equilibrium BEC, the energy spacings between the lowest-lying states determine locally the effect of quantum fluctuations. Our finite size assumption thus models in a simple way the local structure of the spectrum of the disordered system.

Via the Bogolubov ansatz, the exciton and the photon fields are written as

$$\hat{\Psi}_{x,c}(\mathbf{r}, t) = \Phi_{x,c}(\mathbf{r}, t) + \tilde{\psi}_{x,c}(\mathbf{r}, t), \quad (2)$$

i.e. as the sum of a classical symmetry-breaking term $\Phi_{x,c}(\mathbf{r}, t)$ for the condensate wave function, and of a quantum fluctuation field $\tilde{\psi}_{x,c}(\mathbf{r}, t)$. Heisenberg equations of motion result in two coupled equations for $\Phi_{x,c}(\mathbf{r}, t)$. In the HFP approach, anomalous correlations of the excitation field are neglected [15, 16] and we obtain

$$\begin{aligned} i\hbar\dot{\Phi}_x &= \left[\epsilon_0^x - 2\frac{\hbar\Omega_R}{n_s} \text{Re}\{n_{xc} + \tilde{n}_{xc}\} + v(n_{xx} + \tilde{n}_{xx}) \right] \Phi_x \\ &\quad + \hbar\Omega_R \left(1 - \frac{n_{xx}}{n_s} \right) \Phi_c \\ i\hbar\dot{\Phi}_c &= \epsilon_0^c \Phi_c + \hbar\Omega_R \left(1 - \frac{n_{xx} + \tilde{n}_{xx}}{n_s} \right) \Phi_x. \end{aligned} \quad (3)$$

Here, we introduce the density matrix $n_{\chi\xi} = n_{\chi\xi}^0 + \tilde{n}_{\chi\xi}$ ($\chi, \xi = x, c$), where $n_{\chi\xi}^0 = \Phi_{\chi}^* \Phi_{\xi}$ and $\tilde{n}_{\chi\xi} = \sum_{\mathbf{k} \neq 0} n_{\chi\xi}(\mathbf{k}) = \sum_{\mathbf{k} \neq 0} \langle \hat{O}_{\chi}^2(\mathbf{k}) \hat{O}_{\xi}^1(\mathbf{k}) \rangle$ are the contributions from the condensate and from the excited states, respectively. In our notation, $\hat{O}_{\xi}^1(\mathbf{k}) = \hat{O}_{\xi}(\mathbf{k})$ and $\hat{O}_{\xi}^2(\mathbf{k}) = \hat{O}_{\xi}^{\dagger}(-\mathbf{k})$, with $\hat{O}_x = \hat{b}$, and $\hat{O}_c = \hat{c}$. The quantities $n_{\chi\xi}(\mathbf{k})$ are computed self-consistently as described below. By setting $\Phi_{x,c}(t) = e^{-iEt/\hbar} \Phi_{x,c}(0)$ into (3), we obtain a generalized set of two coupled Gross-Pitaevskii equations for the condensate eigenstate. The two solutions of (3) correspond to the lower and upper polariton respectively, and can be expressed as $\Phi_{up(lp)} = X_0^{up(lp)} \Phi_x + C_0^{up(lp)} \Phi_c$, thus fixing the Hopfield coefficients of the polariton condensate. The low-energy solution $E_0^{lp} = \mu$ defines the chemical potential.

In the HFP theory, Eqs. (3) are coupled to the field-equations for excitations. In analogy with the case of a single Bose gas, we define the 4×4 matrix $G(\mathbf{k}, i\omega_n) \equiv \{g_{jl}^{\chi\xi}(\mathbf{k}, i\omega_n)\}_{j,l=1,2}^{\chi,\xi=x,c}$, whose elements are the thermal propagators of the excited particles [16]:

$$g_{jl}^{\chi\xi}(\mathbf{k}, i\omega_n) = - \int_0^{\beta} d\tau e^{i\omega_n \tau} \langle \hat{O}_{\chi}^j(\mathbf{k}, \tau) \hat{O}_{\xi}^l(\mathbf{k}, 0)^{\dagger} \rangle_{\tau}, \quad (4)$$

where $\hbar\omega_n = 2\pi n/\beta$, $n = 0, \pm 1, \dots$ are the Matsubara energies for bosons and $\langle \dots \rangle_{\tau}$ represents the thermal average of the imaginary-time ordered product.

The propagator matrix $G(\mathbf{k}, i\omega_n)$ obeys the Dyson-Belaev equation

$$G(\mathbf{k}, i\omega_n) = G^0(\mathbf{k}, i\omega_n) [\mathbf{1} + \Sigma(\mathbf{k}, i\omega_n) G(\mathbf{k}, i\omega_n)], \quad (5)$$

where $G^0 \equiv \{g_{jl}^0(\mathbf{k}, i\omega_n)\}_{jl}^{\chi\xi} = \delta_{\chi\xi} \delta_{jl} [(-)^j i\omega_n - \epsilon_{\mathbf{k}}^{(\xi)} + \mu]^{-1}$ is the matrix of the unperturbed propagators, and

$$\Sigma(\mathbf{k}, i\omega_n) = \begin{pmatrix} \Sigma^{xx}(\mathbf{k}, i\omega_n) & \Sigma^{xc}(\mathbf{k}, i\omega_n) \\ \Sigma^{cx}(\mathbf{k}, i\omega_n) & \Sigma^{cc}(\mathbf{k}, i\omega_n) \end{pmatrix} \quad (6)$$

is the 4×4 self-energy matrix, here written in a 2×2 -block form. In the HFP limit, the self-energy is independent of frequency and reads

$$\begin{aligned} \Sigma_{11}^{xx} &= \Sigma_{22}^{xx} = 2 \left[v n_{xx} - \frac{\hbar\Omega_R}{n_s} (n_{cx} + n_{xc}) \right], \\ \Sigma_{12}^{xx} &= (\Sigma_{21}^{xx})^* = v \Phi_x^2 - 2 \frac{\hbar\Omega_R}{n_s} \Phi_x \Phi_c, \\ \Sigma_{11}^{xc} &= \Sigma_{22}^{xc} = \hbar\Omega_R \left(1 - 2 \frac{n_{xx}}{n_s} \right), \\ \Sigma_{12}^{xc} &= (\Sigma_{21}^{xc})^* = - \frac{\hbar\Omega_R}{n_s} \Phi_x^2, \end{aligned} \quad (7)$$

while $\Sigma_{jl}^{cx} = \Sigma_{jl}^{xc}$ and $\Sigma_{jl}^{cc} = 0$. For each value of \mathbf{k} , the analytic continuation of the Green's functions $g_{jl}^{\chi\xi}(\mathbf{k}, z)$ have four poles at $z = \pm E_{\mathbf{k}}^{lp(up)}$. They are the positive and negative eigen-energies of the lower- and upper-polariton Bogolubov modes. The components of the corresponding eigenvectors $\mathbf{h}_{\sigma}^i(k) \equiv (X_u, C_u, X_v, C_v)_{\sigma}^i(k)$ ($i = lp, up$ and $\sigma = +, -$) are the generalized Hopfield coefficients of the normal (X_u, C_u) and anomalous (X_v, C_v) kind, with normalization $|X_u|^2 - |X_v|^2 + |C_u|^2 - |C_v|^2 = 1$.

The excited-state density matrix $\tilde{n}_{\chi,\xi}(\mathbf{k})$ is related to the normal Green's functions via the relations

$$\tilde{n}_{\chi\xi}(\mathbf{k}) = \lim_{\eta \rightarrow 0} \sum_{\omega_n} e^{i\omega_n \eta} g_{11}^{\chi\xi}(\mathbf{k}, i\omega_n). \quad (8)$$

The corresponding lower- and upper-polariton densities $\tilde{n}_{lp}(\mathbf{k})$ and $\tilde{n}_{up}(\mathbf{k})$ are obtained from (8) in terms of the generalized Hopfield coefficients. Thus, for a fixed total polariton density n_p , the condensed lower-polariton population is given by

$$n_{lp}^0 \equiv |\Phi_{lp}|^2 = n_p - \tilde{n}_{lp} - \tilde{n}_{up}. \quad (9)$$

From this quantity, Φ_x and Φ_c are finally obtained via the Hopfield coefficients for the condensate X_0 and C_0 , as derived from Eq.(3). Hence, a fully self-consistent solution can be obtained by solving iteratively Eqs. (3), (5), (8), and (9), until convergence of the chemical potential μ and of the density matrix $n_{\chi\xi}(\mathbf{k})$ is reached. From this solution, for a given polariton density n_p and temperature T , we obtain the spectrum of collective excitations $E_{\mathbf{k}}^{lp(up)}$ and the polariton population $n_{lp(up)}(\mathbf{k})$.

For the numerical calculations, we use parameters describing the experiment in Ref. [2], i.e. $\hbar\Omega_R = 13$ meV and detuning $\delta = \epsilon_0^c - \epsilon_0^x = 5$ meV. We study the results as a function of the system area A , ranging from $100 \mu\text{m}^2$ to 1 cm^2 . The momentum-dependent interaction potentials v_x and v_s [17], are evaluated for a CdTe quantum

well. In Fig. 1 we show the energy-momentum dispersion of the collective excitations, $\pm E_{\mathbf{k}}^{lp}$ and $\pm E_{\mathbf{k}}^{up}$, as obtained for two different values of the total polariton density n_p above the condensation threshold, at $T = 20\text{K}$. Close to zero momentum (see inset), the dispersion of the lower polariton branch becomes linear, giving rise to phonon-like Bogolubov modes [5, 20], as in the standard single-field theory [22]. Due to the non-linear terms \hat{H}_x and \hat{H}_s , the polariton splitting decreases for increasing n_p .

The interplay between exciton saturation and interactions in determining the energy shifts has no counterpart in the BEC of a single Bose gas. Here, the two effects produce *independent* energy shifts of the two polaritons. We plot in Fig. 2 (a) the energy shifts of the two polariton modes at $k = 0$, as a function of the density. Exciton saturation and interactions result in a blue-shift of the lower polariton and a red-shift of the upper polariton. The shifts are linear in n_p with the slope changing by a factor of two across the threshold (see inset), because the contribution of the thermal populations \tilde{n}_{xx} , \tilde{n}_{xc} in Eqs. (3) is twice that of the condensed ones n_{xx}^0 , n_{xc}^0 . This trend and the magnitude of the shifts reproduce fairly well the experimental data [2]. To explain the origin of the opposite shifts of the two polaritons, we plot in Fig. 2 (b) the exciton energy $E_0^x \equiv \epsilon_0^x + \Sigma_{11}^{xx}$, and the exciton-photon coupling Σ_{11}^{xc} , as a function of n_p . The two quantities contribute comparably to the deviations from the ideal Bose-gas picture. We predict a very small reduction of the polariton splitting up to the largest polariton density estimated from the experiments, thus supporting the idea that polaritons – as hybrid exciton-photon quasiparticles – are stable well above the BEC threshold.

We now turn to study the thermodynamical properties of polariton BEC. Fig. 3(a) shows the polariton population $n_{lp}(E) + n_{up}(E)$ for two values of the total density n_p , below and above threshold respectively. Below threshold, polaritons follow a Maxwell-Boltzmann distribution. Above threshold, the distribution becomes highly degenerate, with a macroscopic occupation of the lowest-energy state, and a saturation of the population at high-energy. Fig. 3 (b) displays the simulated one-body spatial correlation function $g^{(1)}(\mathbf{r}) = \langle \hat{\psi}_c^\dagger(\mathbf{r})\hat{\psi}_c(0) \rangle / (n_{cc}(\mathbf{r})n_{cc}(0))^{1/2}$ of the photon field. This quantity is directly related, via the photon fraction, to the actual polariton correlation function, and models the outcome of an optical experiment. It shows the occurrence of ODLRO above threshold which is the main feature of BEC of an interacting Bose gas [22]. Below threshold, the correlation extends only over the thermal wavelength $\lambda_T \simeq 1\text{ }\mu\text{m}$. In experiments [2], the correlation pattern is shaped by the interface disorder. However, the measured long-range correlation is always below 40%, as compared to 80% of our prediction. By means of a kinetic model, we have recently suggested [14] that this discrepancy is the main result of deviations from thermodynamical equilibrium, with enhanced quantum

fluctuations depleting the condensate in favor of excitations.

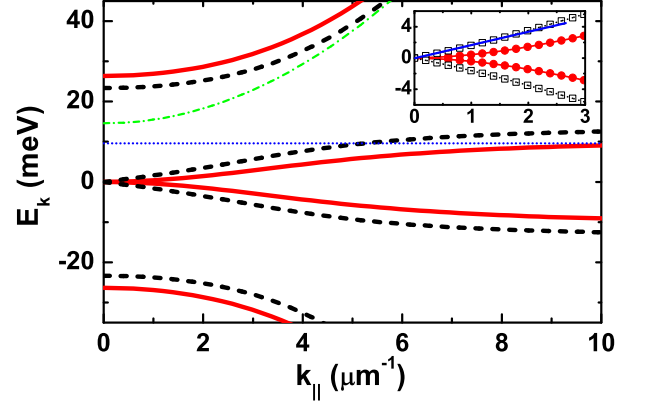


FIG. 1: The dispersion of the normal modes of the system for polariton density $n_p = 15\mu\text{m}^{-2}$ (solid) and $n_p = 400\mu\text{m}^{-2}$ (dashed). The non-interacting photon (dash-dotted) and exciton (dotted) modes are also shown. Inset: detail of the low-energy region, showing the onset of the linear Bogolubov dispersion (the blue straight line is a guide to the eye).

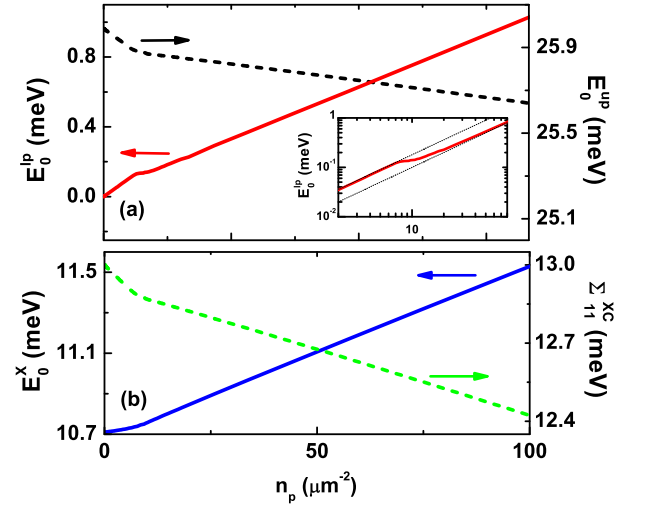


FIG. 2: (a) Lower (solid) and upper (dashed) polariton energies at $k = 0$ vs polariton density n_p . Inset: Double logarithmic plot of the lower polariton energy (dotted lines: linear slopes below and above threshold). (b) Bare exciton energy E_0^x (solid) and effective exciton-photon coupling Σ_{11}^{xc} (dashed). All quantities were computed for $T = 20\text{K}$.

In Fig. 4(a), we report the computed density-temperature phase diagram. In the plot, some values of the exciton fraction $|X_0|^2$ in the polariton condensate are indicated along the phase boundary. It decreases for increasing density, due to interactions, but stays finite, confirming the stability of polaritons up to high density. Fig. 4(b) shows a detail of the low- T region of the phase diagram, computed for different system areas A . We also display the phase boundary of the normal-superfluid

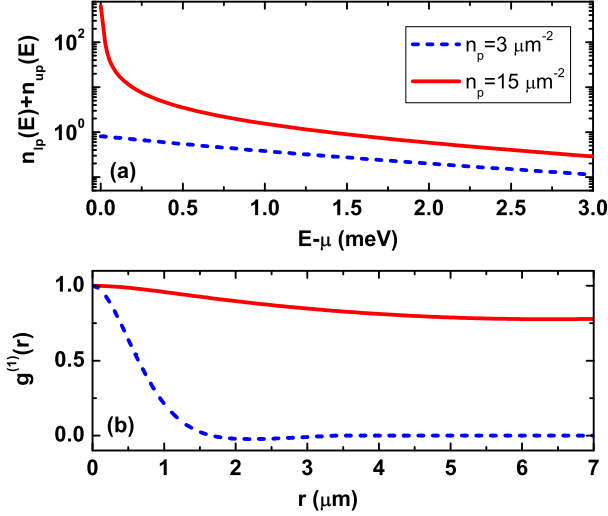


FIG. 3: (a) Polariton population vs. energy for two values of n_p , computed at $T = 20\text{K}$. (b) Corresponding one-body spatial correlation function of the photon field.

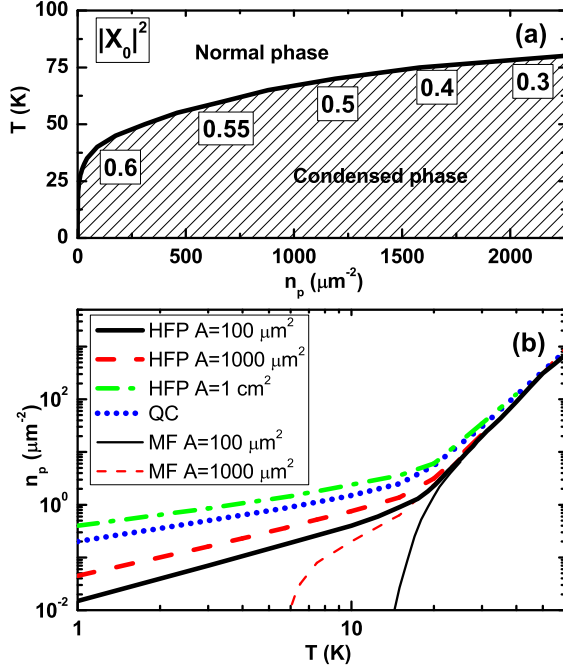


FIG. 4: (a). Phase diagram of polariton BEC, computed for the parameters of Ref. [2], and $A = 100 \mu\text{m}^2$. The exciton fraction in the condensate $|X_0|^2$, along the phase boundary, is indicated in boxes. (b) Detail of the low- T region. HFP denotes the result of the present theory. MF is the mean-field result. QC denotes the quasi-condensate transition, corresponding to the onset of a superfluid density.

(quasicondensate) transition, as obtained from an extension of the Landau formula [22]. For $T < 20\text{K}$ and $A < 1000 \mu\text{m}^2$, the BEC phase boundary lies well below the quasicondensate one. Our BEC picture is thus well suited for the description of recent samples [2, 3], char-

acterized by polariton localization. In the case of a more extended, spatially homogeneous system, a description in terms of the Berezinski-Kosterlitz-Thouless transition would be necessary. Fig. 4(b) also shows the logarithmic increase of the critical density as a function of A , due to the increase of thermal fluctuations. Quantitatively, the variation is very small, in particular for $T \geq 20\text{K}$ [2]. This dependence and the quasicondensate behaviour are hence only expected in samples with improved interface quality and at lower temperature. The thin lines in Fig. 4 (b) are the result of a mean-field approximation, obtained by neglecting the excited states population, i.e. $n_{lp}^0 + n_{up}^0 = n_p$. This approximation overestimates the group velocity at $k = 0$, thus strongly underestimating the critical n_p at low T . This points out to the importance of the HFP approach that we have adopted.

In conclusion, we have generalized the HFP theory to the case of two coupled Bose fields at thermal equilibrium. The theory allows modeling the BEC of polaritons in semiconductor microcavities in very close analogy with the BEC of a weakly interacting gas. The predicted critical density is in good agreement with a recent measurement [2]. Our analysis thus supports the interpretation of the experimental findings in terms of a transition to a quantum degenerate Bose fluid. Open questions remain, basically related to the role of disorder and localization. If the sample quality can be improved, polaritons will become an invaluable tool for studying the effects of dimensionality and fluctuations in interacting Bose systems.

* davide.sarchi@epfl.ch

- [1] H. Deng *et al.*, PNAS **100**, 15318 (2003).
- [2] J. Kasprzak *et al.*, Nature **443**, 409 (2006).
- [3] H. Deng *et al.*, Phys. Rev. Lett. **97**, 146402 (2006).
- [4] J. Keeling, Phys. Rev. Lett. **93**, 226403 (2004).
- [5] F. M. Marchetti *et al.*, Phys. Rev. Lett. **96**, 066405 (2006).
- [6] M. H. Szymanska *et al.*, Phys. Rev. Lett. **96**, 230602 (2006).
- [7] A. Kavokin *et al.*, Phys. Lett. A **306**, 187 (2003).
- [8] J. Keeling, Phys. Rev. B **74**, 155325 (2006).
- [9] F. P. Laussy *et al.*, Phys. Rev. Lett. **93**, 016402 (2004).
- [10] T. D. Doan *et al.*, Phys. Rev. B **72**, 085301 (2005).
- [11] D. Sarchi and V. Savona, phys. stat. solidi (b) **243**, 2317 (2006).
- [12] P. Schwendimann and A. Quattropani, Phys. Rev. B **74**, 045324 (2006).
- [13] M. Wouters and I. Carusotto, ArXiv:cond-mat/0702431.
- [14] D. Sarchi and V. Savona, Phys. Rev. B **75**, 115326 (2007).
- [15] A. Griffin, Phys. Rev. B **53**, 9341 (1996).
- [16] H. Shi and A. Griffin, Phys. Rep. **304**, 1 (1998).
- [17] G. Rochat *et al.*, Phys. Rev. B **61**, 13856 (2000).
- [18] S. Ben-Tabou de-Leon and B. Laikhtman, Phys. Rev. B **63**, 125306 (2001).
- [19] S. Okumura and T. Ogawa, Phys. Rev. B **65**, 035105 (2002).

- [20] I. A. Shelykh *et al.*, Phys. Rev. Lett. **97**, 066402 (2006).
- [21] S. Schmitt-Rink *et al.*, Phys. Rev. **B 32**, 6601 (1985).
- [22] L. Pitaevskii and S. Stringari, *Bose-Einstein condensation* (Oxford University Press, 2003).
- [23] M. D. Lee *et al.*, Phys. Rev. A **65**, 043617 (2002).
- [24] Estimated from a kinetic model [14]. For this lifetime, also the excitation spectrum should tend to the equilibrium one, as can be seen from Eqs. (8)-(10) of Ref. [13].
- [25] We assume scalar exciton and photon fields. The theory can be generalized to include their vector nature, accounting for light polarization and exciton spin, as done by Shelykh *et al.*, within the Gross-Pitaevskii limit [20].
- [26] In 2-D, many-body correlations affect significantly the two-body scattering amplitude, eventually leading to a vanishing T -matrix at small collision energy and in the thermodynamic limit [23]. In the HFP approximation, it is then customary to replace the interaction potential $v(\mathbf{k}, \mathbf{k}', \mathbf{q})$ by the many-body T -matrix $T(\mathbf{k}, \mathbf{k}', \mathbf{q}, E)$ obtained from a self-consistent summation of ladder diagrams. Here, we have generalized this approach and computed the many-body T -matrices $T_x(\mathbf{k}, \mathbf{k}', \mathbf{q}, E)$ and $T_s(\mathbf{k}, \mathbf{k}', \mathbf{q}, E)$. We find that, for typical parameters, the correction to v_x and v_s is of only a few percent.